Evaluation of the Structural Behavior of Prestressed Concrete Bridge Girders under Diagnostic Load: A Test-Case Study

Oday A. Abdulrazzaq
Department of Civil Engineering, College of Engineering, University of Basrah, Basrah, Iraq
oday.abdulrazaq@uobasrah.edu.iq

Jaffar A. Kadim
Department of Civil Engineering, College of Engineering, University of Basrah, Basrah, Iraq
jaffar.kadhim@uobasrah.edu.iq (corresponding author)

David Abed Mohammed
Department of Civil Engineering, College of Engineering, University of Basrah, Basrah, Iraq
david.jawad@uobasrah.edu.iq

Received: 11 January 2025 | Revised: 7 February 2025 and 20 February 2025 | Accepted: 22 February 2025

 DOI: https://doi.org/10.48084/etasr.10196

ABSTRACT

This study deals with the structural behavior of prestressed concrete bridge girders consisting of 4 spans using the field diagnostic load test method and comparing the results with the mathematical model of the CSiBridge program. The bridge under study is located in the city of Basra in southern Iraq and was constructed more than 40 years ago, which makes it necessary to determine the actual structural conditions in order to decide whether it is safe to keep using it or not. A 48.5 tn vehicle was used for the test, where each area was divided into 3 load paths, and then the site data values were simulated utilizing the CSiBridge program. The field test data cleared the durability of the bridge for all spaces from any structural defects, and the correlation test results were very close with the analytical study results. The field results indicate that half of the lanes tested behave linearly and the other half behave non-linearly, with the source of the non-linearity being related to the potential problems of the prestressed girders. The theoretical results also proved that vehicles with a load of 72.4 tn can go through, without causing any damage to the different parts of the bridge.

Keywords-bridge loading test; diagnostic load test; proof bridge test; Prestressed Reinforced Concrete (PRC) girder; bridge rating; CSiBridge program

I. INTRODUCTION

For nearly the entire 20th century, prestressed concrete girder bridges have been widely constructed, due to their simplified design and the least formwork requirements compared to the reinforced concrete bridges. In Iraq, simple-support prestressed concrete girders have been mainly adapted in the last decades for 2 to 6-span configurations with lengths of 18 m to 36 m. There is little documentation of the design and construction of these bridges, and many of them are still in moderate to good condition (adequate service, performance, and appearance). Consequently, a comprehensive evaluation of the current state of these bridges is necessary, noting that the visual inspection and/or conventional analytical methods are not sufficient to answer the potential behavioral problems (material and structural behavior) related to these bridges after passing 40 years from their constriction. In addition, an accurate assessment of both their material composition and load-bearing capacity is important. In situ testing is a methodical and quantitative method pattern, used to determine the strength of the bridge. The diagnostic load test is classified as a non-destructive load test because the applied load does not reach the ultimate bridge capacity, but it is applied by finding the Rating Factor (RF) as specified in the ASSHTO standard [1]. A common practice involves comparing the test bridge's results with theoretical models developed using Finite Element Method (FEM) software, such as CSiBridge, to ascertain the coefficient of correlation between the two types of results. Ultimately, the rating process is derived from the relationship between both destructive and nondestructive tests. The diagnostic load test has a variety of applications including verifying the specific characteristics of bridge elements and comparing the test results with the structural analysis results. It can also provide information on the relationship between

various parameters, such as load and stress. Therefore, it is possible to estimate the actual ultimate strength of the tested bridges providing a straightforward assessment of the new applying vehicle load, considering the benefits of the rating procedure to assess the carrying load capacity. This procedure also allows for the determination of load limits. Typically, the available equipment is used in conjunction with current illustration inspections to facilitate more informed decisions regarding the particular bridge under consideration. The estimate of bending is a critical concept in the test, while sometimes an additional strain sensor can be used to assess the rotations at specific locations. The results of the loading test can be used to study the strength and behavior of different bridge members. Through the load test, different patterns may be evaluated as acceptance limits and procedures to show the engineering conclusion in the strength estimation and to ensure that the bridge elements do not have major defects. Authors in [2] conducted a substantial number of bridge load tests, with one notable example being a destructive loading test on short-span reinforced concrete bridges. This test involved the usage of a single dump truck to assess the load rating of 20 short-span reinforced concrete bridges. A wide range of parameters, such as span length, span width, skew angle and parapet type have been examined to reach the general theory for these types of bridges. Authors in [3] tested the static loading of three bridges in Costa Rica using truck weights (25,960 tn to 27,285 tn) as test loads. The deflection of the bridge girders and the stress of the steel members of the bridge were utilized as criteria to identify the girder response during the loading test. The findings from this study were then used to determine the maintenance method for repairing the tested bridges. Authors in [4] deployed a recently constructed segmental concrete bridge in the surroundings of Žilina city as a case study. This bridge was made of two box prestressed girder structures, which were designed employing the balanced self-supporting method. The bridge's total length is 1,042 m, distributed across 18 spans, with the main spans measuring 60.5 m. Prior to its operation, the bridge's construction process and load-bearing capacity (including bridge monitoring) were examined. The bridge's behavior was analyzed under the effect of static load, followed by comparisons with the predicted model for both cases, as the prestressed and precast. Authors in [5] examined an existing bridge with limited data concerning its construction state, using a proof load test to ascertain the bridge's load-bearing capacity, as outlined in AASHTO standard [1]. The obtained results indicated that the magnitude of the target load, as specified by the proof Load Factor (LF), was directly related to the desired level of reliability. Authors in [6] proposed a multiagent-based system that contains deep knowledge backup for improving the monitoring of a bridge's crossing traffic. This occurs through the employment of a new system for monitoring autonomously crossing vehicles in real time to avoid the hastening of a bridge's infrastructure decline. The projected system has the potential to enhance driver safety, reduce maintenance costs, provide insights into bridge collapse, and extend bridge lifespans. Following a period of over 40 years, an evaluation process was deemed necessary for the bridge under study in Basra City, southern Iraq. This decision was taken due to the passage of loads weighing 60 tn, and the luck of any previous maintenance processes, rendering the evaluation of the bridge's structural behavior under a similar type of load necessary. The load test can be used to determine the cause of any found defects and cracks, determining the concretes' condition, and extending any of the horizontal cracks visible on both sides of the deck. Additionally, the nature of the existing flexure and shear stiffness can be ascertained through a comparison with the current load rating conducting a diagnostic load test in lieu of a maximum load test, not only for safety reasons, but also due to the loss of all design documents pertaining to the bridge's design and construction. A detailed survey of the bridge site was conducted in December 2022, following the collection of geometry measurements and the performance of engineering tests, showing that the bridge was in good condition, with no damage to the main deck, making it possible to carry out a diagnostic load test of the bridge with a 48.0 tn vehicle. The development process involves two stages. The first entails comparing the response of the bridge under load test with the mathematical model through the CSiBridges program, while the second stage includes determining the RF according to the ASSHTO standard [1] from the CSiBridge results.

II. BRIDGE CHARACTERISTICS

In 1980, the bridge under investigation was constructed, consisting of four simply supported spans that were PRC girder (a 15° skew) located in Basra City, Southern Iraq. The deck comprises a reinforced concrete slab measuring 200 mm in thickness, cast with PRC girders that are supported by square elastomeric bearing pads measuring 400 mm ×400 mm ×50 mm. The total bridge length is 72.4 m, with equal spans of 18.0 m. The overall bridge width is 12.4 m, and the face-to-face distance between parapets is 12.0 m, as seen in Figure 1. The number of PRC girders in the outer spans is 17, while in the inner spans are 13. The abutments and piers are continuous beams cast along the bridge width to support all girders bearing a width of 1.2 m, a length of 12.4 m, and a height of 3.5 m, which rest on precast pile foundations. Prior to the diagnostic load test, two types of tests had been conducted. The first was a visual examination, which revealed that the bridge deck was intact and free of any defects or cracks.

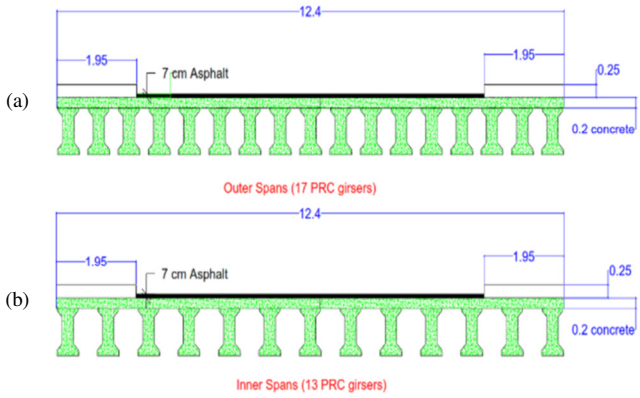

Fig. 1. Bridge deck geometry details (dimensions in m): (a) outer spans, (b) inner spans.

However, it was observed that there were minor horizontal hairline cracks in the piers, particularly in the center of each external pier. The second type of test involved the determination of various engineering properties of the concrete and reinforcing steel. The rebound hammer and ultrasonic pulse velocity tests were conducted in accordance with ASTM C805 and C597, respectively, to assess the compressive strength of concrete across various bridge elements. The outcomes of these evaluations revealed that the cube compressive strength of PRC girders, deck slabs, and piers and abutments were found to be 45 MPa, 32 MPa, and 25 MPa, respectively. The half-cell potential test was conducted in accordance with ASTM 876 to ascertain the presence of corrosion in the reinforcing bars. The test results indicated an absence of corrosion in any region of the bridge.

III. DIAGNOSTIC TEST

The test is based on three steps: specification of the vehicle type used in the test, determination of the load paths, and establishment of the test procedure protocol.

A. Tested Load

The primary objective of a bridge assessment is to ascertain the load capacity that the bridge can sustain without experiencing serious deficiencies and/or damage that would pose a hazard to vehicles or persons. It should be noted that the possible future deterioration of the bridge is not included in the test and the diagnostic load test is conducted by a 48.5-ton trailer-tanker, as shown in Figure 2. This is similar to or higher than the load used for the maximum serviceability limit state. Additionally, Figure 2 presents the surveyor's position relative to the bridge span under evaluation for which the recording device boasts an accuracy of 0.1 mm.

Fig. 2. Test vehicle.

B. Load Paths

In order to test all possibilities of vehicle passage over the tested bridge spans, three load paths are created prior to the test for the driver to follow, which are designed to produce maximum response. Two lanes are created as close to either side of the guardrail as the driver can position the vehicle, and one lane is created in the center of the bridge, as portrayed in Figure 3. The deflection measurement points are attached to the lower surfaces of the centers of all lanes at the bottom of girder numbers 4, 7, and 10 (for spans 2 and 3) and at the bottom of girder numbers 5, 9, and 13 (for spans 1 and 4).

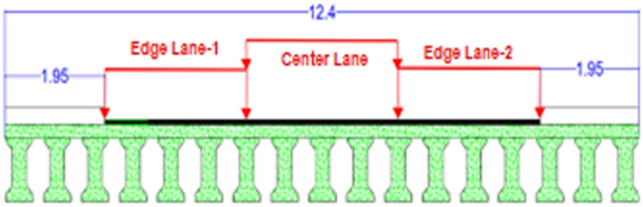

Fig. 3. Transverse positions for test vehicle (dimensions in).

C. Test Procedure

Many codes of practice and test reports are applicable when conducting the diagnostic load test [7]. The following procedure is used for each path tested in all four bridge spans, noting that the bridge must be cleared of all traffic prior to the test initiation. First, the load test involves the passage of a single test vehicle (5-axle water tanker weighing 48.5 tons), noting that the tests are conducted with the test vehicle travelling along the bridge at a crawl speed of 5km/hr. Secondly, the test starts when the front axle of the test vehicle enters the first span of the bridge and terminates when the rear axle exits the end span. Then, the traffic is free to flow once the rear axle of the test vehicle exits the testing region. The average time required for vehicle passage along each transverse position ranges between (30 sec- 2 min) depending on the bridge span. Finally, the test readings were taken on the underside of the bridge, using an optical digital level situated in the surrounding area, approximately 30m from the bridge.

IV. ANALYTICAL STUDY

Theoretical studies have been used for two purposes: the validation checking of the diagnostic test results and the bridge rating, which is related to the determination of the maximum safe load that can be applied to the passing vehicles. The analysis, design, and rating of the tested bridge were accomplished using CSiBridge Version 21. Given that each span of the tested bridge consists of a simply supported deck, with the deck slab being separated by expansion joints, the analysis is achieved by one span of two models, 13 girders and 17 girders. Furthermore, the study includes the definition of the lane layout (three lanes: right, center, and left), and the material and member definitions obtained from the in-situ test and field measurements, such as the main girder dimensions for the inner and outer spans, as shown in Figure 4. Subsequently, the superstructure and substructure of the bridge will be built, including the slab-girder deck (prestressing tendon properties), abutments, piers, bearings, and foundations. A critical step in this process is the definition of the vehicle class and the vehicle load. The present study relies on FM 55-30 [8], which specifies the load ratio of five vehicle axles as 14%, 20%, 20%, 23%, and 23%, respectively, which is equal to 6.78 tn, 9.68 tn, 9.68 tn, 11.13 tn, and 11.13 tn, as illustrated in Figure 5, where the spacing between the five axles is also demonstrated. Subsequently, two load cases are created, including the dead load case (consisting of the weight of the deck, wearing surface asphalt, and pavement) and the live load case (vehicle load).

The bridge is then evaluated according to the report of the JICA team [3], analyzing the design process according to the AASHTO standard [9].

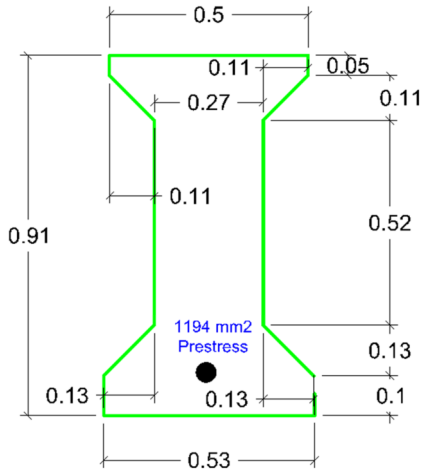

Fig. 4. Main girder geometry (dimensions in m).

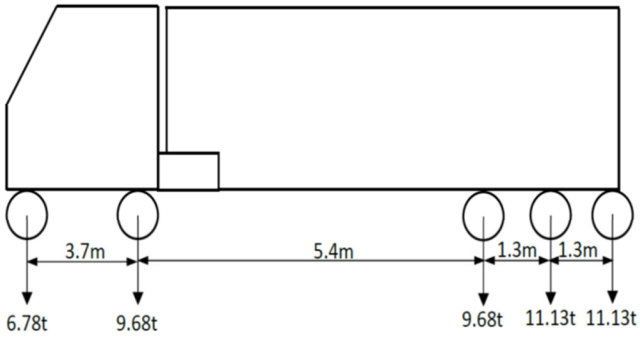

Fig. 5. Test vehicle axle loads and spacing.

Finally, the drawing of the CSiBridge program of the outer span formulation (17 PRC girders) is displayed in Figure 6. The safe load carrying capacity of a bridge is expressed as an RF of a defined vehicle. Typically, an RF ≥ 1.0 signifies sufficient live load carrying capacity, whereas an RF < 1.0 indicates inadequate live load capacity. The AASHTO Manual for Bridge Evaluation (MBE) [1] specifies that each highway bridge should be evaluated at two levels, inventory and operational. The calculation of inventory rating is exclusive to cases of design live loads for which the bridge is intended. It is defined as the design load level that can be safely used for an indefinite period of time. Operating rating is determined for design live loads, legal loads, and permit vehicles. It is defined as the absolute maximum load level to which a bridge structure may be subjected. The Load Factor (LF) method is employed to evaluate the bridge under multiples of the actual loads (factored loads). A multitude of parameters are deployed for both categories of loads to account for the inherent uncertainty in load calculations. The bridge rating is determined so that the effect of the factored load is not greater than the strength of the member. The load rating of the structure is determined by the following general expression:

$$RF = \frac{C - A_1 D}{A_2 L(I+1)} \quad (1)$$

$$RT = RF \times W \quad (2)$$

where RF is the live load RF for the carrying capacity, C is the capacity of the member, D is the dead load effect on the member, L is the live load effect on the member, I is the impact factor to be used with the live load, A_1 is the factor for dead loads, A_2 is the factor for live load, RT is the bridge member rating (tn), and W is the weight of nominal truck used in determining the live load effect, L (tn). For the LF method, A_1 = 1.3 and A_2 changes according the desired level of rating. For the inventory level, A_2 = 2.17 and for the operating level, A_2 = 1.3.

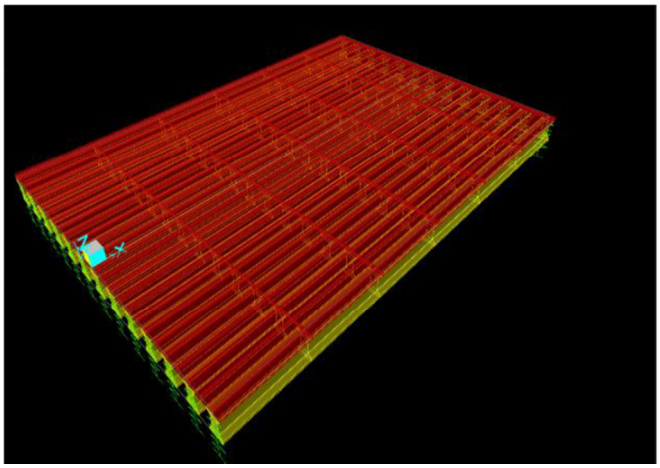

Fig. 6. Finite element of the outer span model.

V. RESULTS AND DISCUSSION

The results of the analytical study and field load test of the aforementioned bridge can be summarized as:

A. Maximum Deflection

The values of the mid-span deflection that were measured and the results of the FEM, which were obtained using the CSiBridge 21 software, are shown in Table I.

TABLE I. MID-SPAN DEFLECTIONS FROM THE DIAGNOSTIC LOAD TEST AND FEM METHOD (VALUES BETWEEN BRACKETS)

Span	Vehicle path	Mid-Span deflection (mm)		
		Right	Centre	Left
1	Right	21.0 (6.1)	18.0 (3.8)	1.7 (0.3)
	Central	15.4 (4.1)	21.0 (6.2)	17.7 (4.1)
	Left	1.4 (0.5)	14.9 (4.8)	18.0 (6.5)
2	Right	5.3 (4.1)	1.3 (1.2)	1.1 (0.9)
	Central	4.1 (2.0)	5.6 (3.7)	0.7 (2.6)
	Left	1.6 (0.2)	3.3 (2.0)	16.1 (6.4)
3	Right	8.0 (6.2)	3.8 (2.5)	2.9 (1.1)
	Central	2.9 (2.7)	22.1 (6.6)	6.3 (3.0)
	Left	1.3 (0.4)	3.0 (1.9)	16.1 (6.3)
4	Right	7.4 (6.5)	3.7 (3.3)	2.8 (0.6)
	Central	0.9 (2.2)	5.6 (5.0)	2.5 (2.2)
	Left	1.3 (0.4)	3.6 (2.5)	5.4 (5.1)

It is evident that the field deflection results are below the limit specified by the AASHTO specifications [3, 9] (L/800 = 18000/800 = 22.5 mm), which leads to one of the most important issues. That is, the diagnostic test meets the serviceability requirements for all spans. The results outline the difference between the deflection values in the left and right samples, despite the fact that both the vehicle load and the beam geometry are the same. The primary cause of these variations is related to the differences in the modulus of elasticity calculated directly from the in-situ compressive stress test for both the deck slab and the prestressed concrete girders, which have variation values related to each girder. In specific, taking span 1 as an example, the cylinder strength of the right and left girder portions are 35.0 MPa and 32.6 MPa, respectively, which are given the concrete elastic modulus of 28000 MPa and 27023 MPa. The ratio between the elastic modulus is (27023/28000=0.96), which is identical to the ratio of the deflection values of the two patterns (6.1/6.5=0.96). The second point concerns the variation of the diagnostic results that reflected the actual condition of the bridge component. Prior to analyzing the underlying causes of the field results, it is noteworthy that the bridge tests (specifically, the 12-load vehicle test) revealed no settlement in the pile cap of any of the piers or two abutments, nor in the bridge bearing. Consequently, the recorded deflection during the test is indicative of the deflection of the girders. Additionally, the test yielded no defects in any of the bridge components, including but not limited to cracks, debonding, and permanent deflection after the vehicle passed. The deflection variation values of the outer spans range from very small, for example for the central path vehicle load as in span 4 (5.6 mm), to large values, as in span 1 (21.0 mm), and similarly for the inner spans, as in span 2 (5.6 mm) compared to span 3 (22.1 mm). In order to compare the difference between the linear response and the nonlinear response, it is important to note that the CSiBridge results show only the linear response. The presence of nonlinear behavior may be caused by many factors that work together to produce the final effects, and these effects are not included in the CSiBridge software. Some causes of the nonlinearity can be related to the creep and fatigue effects on the concrete, which can be seen from the differences of all site deflections of smaller values, rather than the CSI Bridge deflections, as in the span 4 results. Additionally, the repeated passage of heavy vehicles over many decades has the potential to induce various problems in bridge decks, such as internal cracks (non-visible inelastic cracks, slip deformations among bridge deck elements, etc.), which may result from unexpected loading conditions, including impact load, sudden brake load, and prolonged stopping of vehicles on the bridge. Furthermore, the condition of prestress tendons over time following their construction, involving interlocking with concrete and other tendon loss types, is a matter of concern due to their undetermined values and random distribution. Figure 7 illlustrates the distribution of linear and nonlinear behaviors of the bridge under consideration, as measured across three distinct paths. The linear bridge deck behavior accounts for 50% of the entire bridge loaded decks. The left path exhibits a higher degree of nonlinearity behavior, primarily due to the fact that the majority of vehicles travelling at full load are passing through this route. The third point relates to the comparison of the diagnostic results with the CSiBridge results for all bridge spans in order to validate the bridge finite element models for further analysis. Therefore, the correlation study is performed between the two sets of maximum deflections obtained from the field load test and the FEM, respectively.

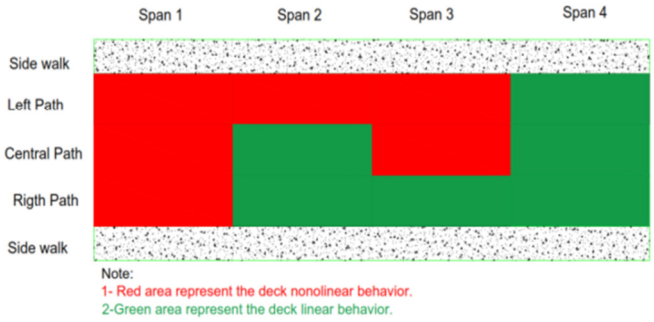

Fig. 7. The linear and nonlinear deck behavior for all spans and paths.

The correlation coefficient (R), which quantifies the strength of the relationship between two or more sets of data, is calculated for all bridge spans, as outlined in Table I. As a result of the value of the correlation coefficient shown in Figure 8 (R=0.7) and using Table II, which indicates that the high positive relationship is present between the field test and analytical data tested bridges [10], it is practical to apply the models to perform further stress analysis and evaluate the bridge RFs.

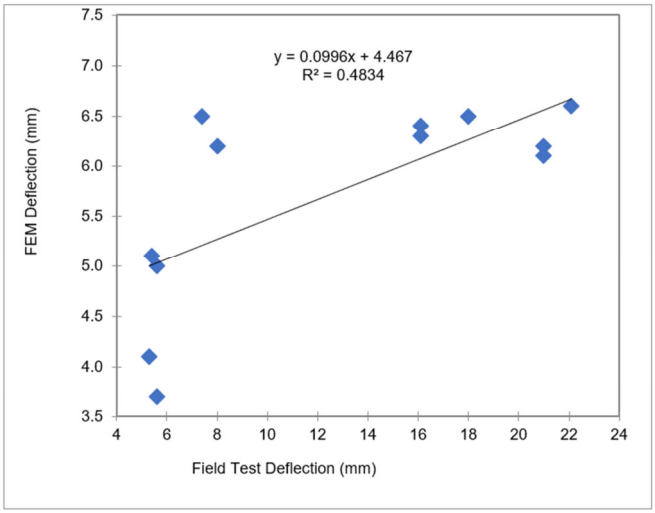

Fig. 8. Linear correlation graph for bridge 4 between the diagnostic test and FEM CSiBridge results.

TABLE II. RULE OF THUMB FOR INTERPRETING THE SIZE OF A CORRELATION COEFFICIENT

Size of correlation	Interpretation
0.90 to 1.00 (–0.90 to –1.00)	Very high positive (negative) correlation
0.70 to 0.90 (–0.70 to –0.90)	High positive (negative) correlation
0.50 to 0.70 (–0.50 to –0.70)	Moderate positive (negative) correlation
0.30 to 0.50 (–0.30 to –0.50)	Low positive (negative) correlation
0.00 to 0.30 (0.00 to –0.30)	Negligible correlation

B. Distribution of Deflections

The benefits of the recorded deflections and FEM results at the middle span are examined, along with the effects and causes of the nonlinear bridge deck behavior, checking the bond condition between the slab deck and PRC girders. The initial step involves the graphical analysis of the deflection values of Table I in relation to spans 1 and 4, noting that spans 2 and 3 have a combined behavior that does not indicate a clearance indication.

Figure 9 shows the lateral distribution of the maximum deflections of bridge girders at the midpoint of span 1 for the three paths, while Figure 10 presents analogous results for span 4. The FEM results, which represent linear behavior, are plotted as solid lines, while the test results, which represent nonlinear behavior, are plotted as dashed lines. The curves of the lateral distribution of the maximum deflection values for span 1 are downward concave for both the FEM and test results and the central path for span 4 is down concave, while the curves of the right and left paths are up concave.

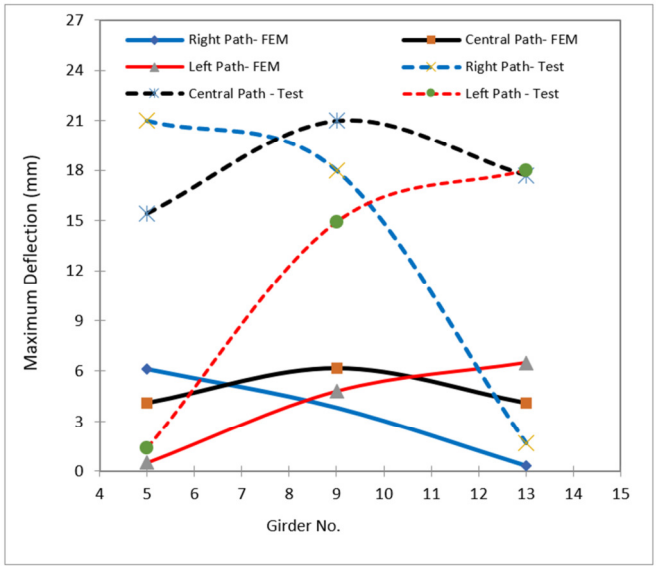

Fig. 9. Bridge deflections at centers of three paths in the middle of span 1.

It is evident that, in the linear analysis employed in the FEM using the elastic theory, the structural response of the bridge girders (i.e., the bending moment, shear force, and load participation) is directly proportional to the maximum deflection at the mid-span of the simply supported deck. Consequently, the lateral distribution of the load transferred from the vehicles via bridge girders is directly associated with the maximum deflection for the FEM results, as presented in Figure 10, which corresponds to span 4, when compared with the vehicle test results. This is achieved by comparing the ratio of the maximum deflection to other values along the cross girders. For span 4, using the test results, the ratio of the load transferred to the center and left girder compared to the right girder is 3.7/7.4=0.50 and 2.8/7.4=0.38 for the right path of the loading case, while for the FEM results, these ratios become 3.3/6.5=0.51 and 0.6/6.5=0.09. In the case of the left loading path, the ratios of the load transferred compared to the left girder are 0.67 and 0.24, respectively, for the central and left paths, while the ratios for the FEM results are 0.49 and 0.08, respectively. However, the nonlinear behavior exhibited different characteristics. The results of the span 1 test are correlated with the ratio of the deflections of the right load path 18.0/21.0=0.86, 1.7/21.0=0.08, while for the FEM results these ratios become 3.8/6.1=0.62 and 0.3/6.1=0.05. The nonlinear behavior of the bridge is influenced by its degree of nonlinearity, as indicated by the ratio of deflections of the right loading path 18.0/21.0=0.86, 1.7/21.0=0.08, and the FEM results 3.8/6.1=0.62 and 0.3/6.1=0.05. The test results for the left loading path 14.9/18.0=0.83, 1.4/18.0=0.08, and the FEM results 4.8/6.5=0.74, 0.5/6.5=0.08 also demonstrate this behavior.

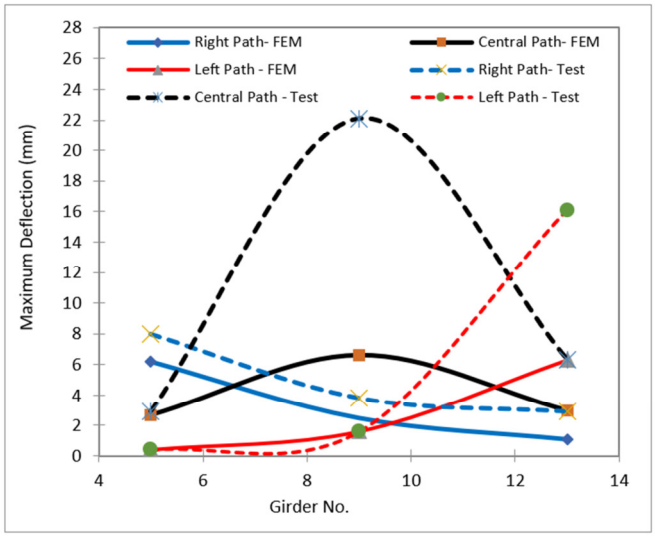

Fig. 10. Bridge deflections at centers of three paths in the middle of span 4.

Consequently, the nonlinear effect on the lateral distribution of loads is causing an increase in the load transferred to the adjacent bridge girders compared to that resulted from FEM (linear effect). Accordingly, the ratio of loads transferred to the central girders is higher than that transferred to the adjacent girders, whether the load was applied on the left or right lanes. In accordance with the above results, there are two probabilities to define the nonlinear behavior of the bridge deck during the diagnostic test. The first possibility is the partial loss of the bond between the RC slab and PRC girders, while the second is the potential problems related to the PRC girder. In the case of direct vehicle load application to the deck, from the vehicle tires to the asphalt wearing surface, and subsequently transferring loads to the PRC girders located beneath the vehicle, the PRC girders receive the greater amount of vehicle load. Then due to the linear behavior, the adjacent PRC girder will receive a load via the linear deflection ratio as its locations are deflected by the vehicle. In the initial probable scenario (bond loss), the vehicle's main load remains in the lane of vehicle loading, resulting in the PRC girders located beneath the vehicle, being deflected to a greater extent than all other deck girders by a significant margin. This is due to the absence

of shear stress between the RC slab and PRC girders. Consequently, the girders near the loading lane will not share the vehicle load, thereby minimizing the recorded deflection. In addressing the second issue, it is crucial to note that the PRC girders will bear the predominant share of the applied load. Due to their inherent nonlinear characteristics, these girders will increase their deflection values, which will force the adjacent lane PRC girders to deflect as the full bond between the RC slab deck and the PRC girders exists. The deflection of the adjacent lane girders is caused by two factors: the linear action of the full bond between the RC slab deck and PRC girders of the loaded lane and the nonlinearity of their PRC girders. It is observed that both lanes (the loaded lane and the adjacent lanes) for the left and right load paths are shared by 92% of the applied vehicle load, while the far-end lanes (the left lane in the right load path and the right lane in the left load path) are only 8% of the applied load vehicle. This results in the remaining lanes behaving linearly due to this small load portion. It is evident that the origin of bridge deck nonlinearity is attributable to PRC girders, rather than to the degradation of the bond between the deck slab and PRC girders. The nonlinearity phenomenon appears to occur in all paths of span 1 in the same manner.

C. Bridge Rating

Table III provides the design factors controlled by the flexural capacity of the bridge spans that meet the serviceability criteria (RF>1.0) for the specified load. The maximum vehicle load that can be applied to bridge No. 4 is equal to: 48.6 × 1.5 = 72.9 tn.

TABLE III. BRIDGE RFS

Span	Limiting capacity	Inventory RF	Operating RF
Outer spans (1 and 4)	Flexure	1.78	2.97
Inner spans (2 and 3)	Flexure	1.50	2.50

The RFs for the bridge under study are calculated using the CSiBridge software, as presented in Figures 11 and 12. Figure 11 shows the bending capacity (critical condition in terms of shear and torsion capacity) for the bridge spans 1 and 4, while Figure 12 presents the bending capacity for the bridge spans 2 and 3

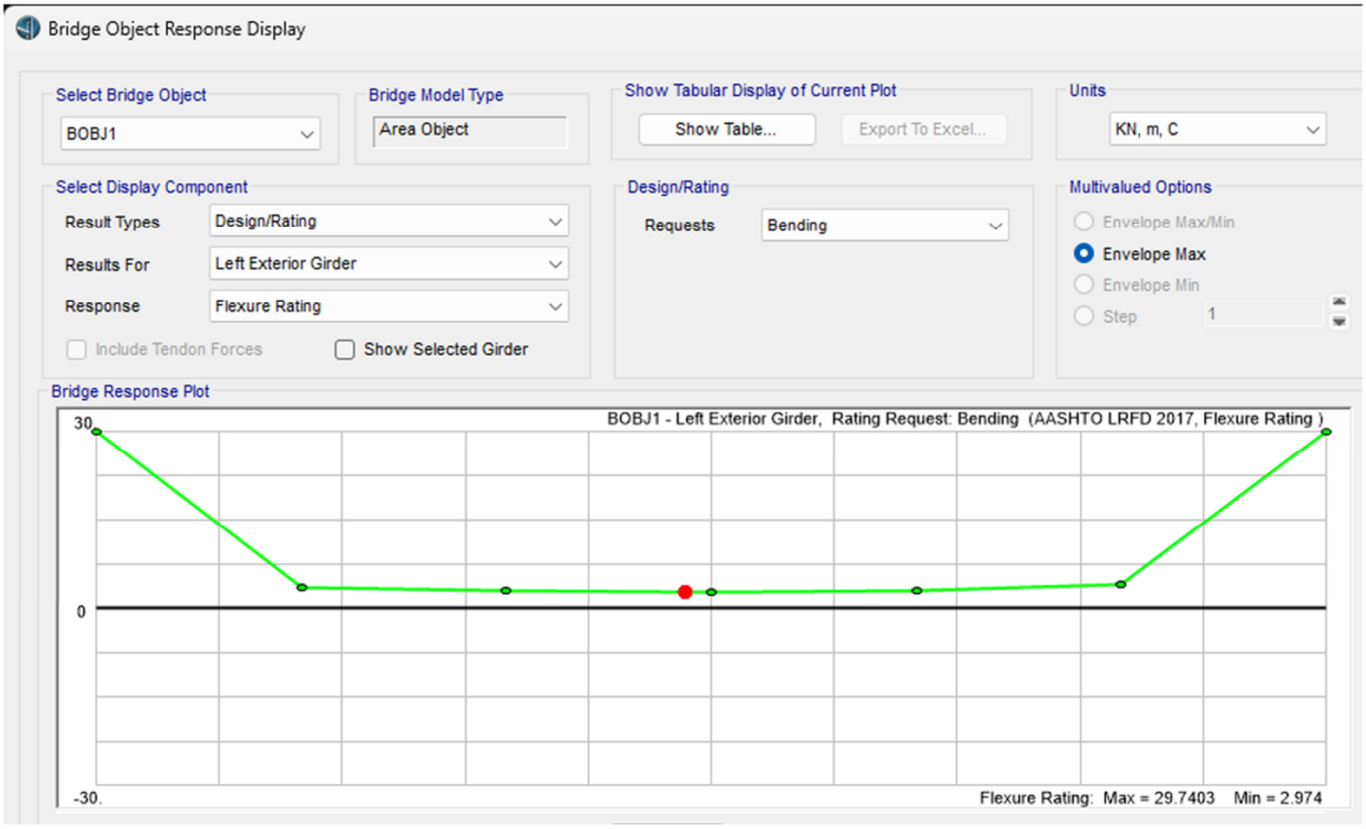

Fig. 11. Rating for bridge spans no. 1 and 4.

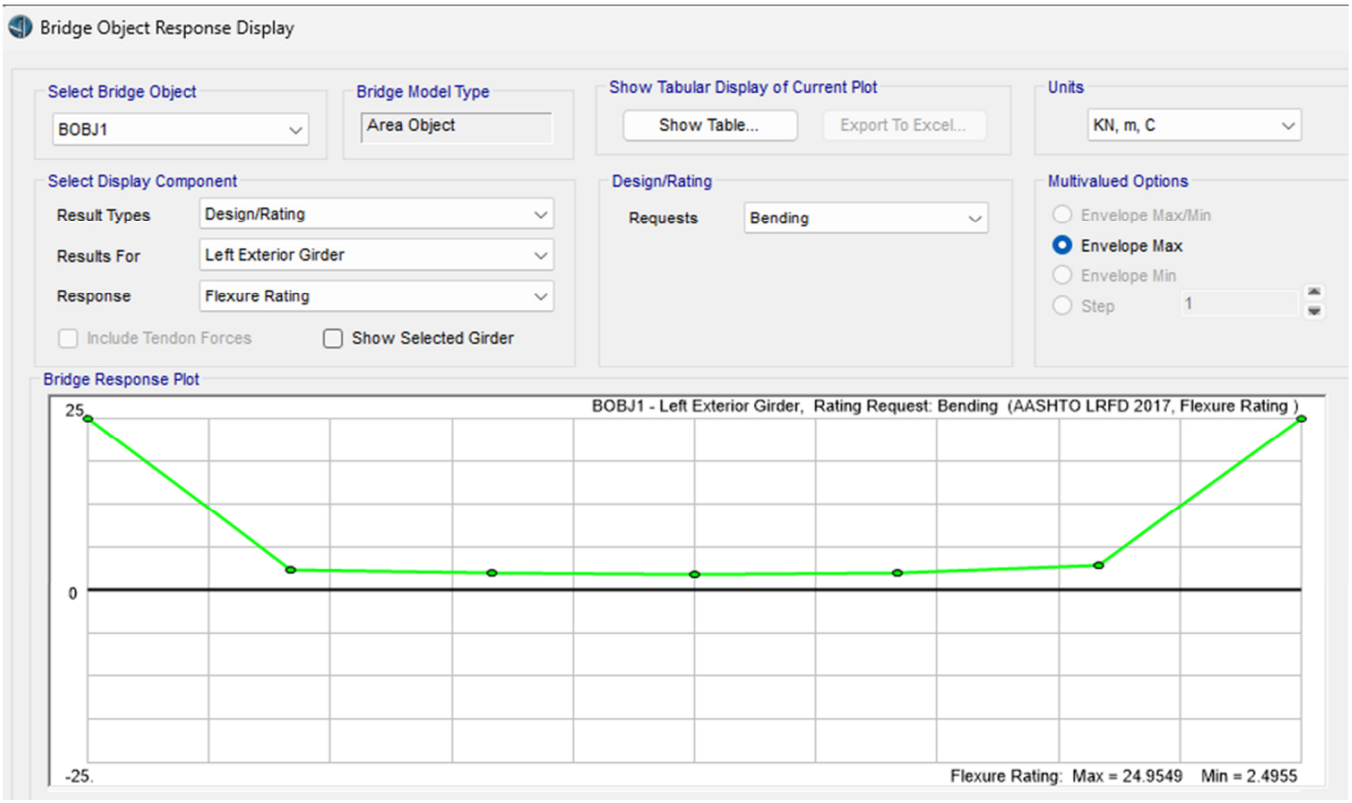

Fig. 12. Rating for bridge spans no. 2 and 3.

VI. CONCLUSIONS

A thorough examination of the obtained results reveals that:

- 12 diagnostic load tests were successfully conducted for 4 spans of the bridge under study, each of which was divided into three loaded lanes.
- The theoretical analysis was carried out using CSiBridge software, which indicates a strong correlation with the results of the diagnostic load test.
- The field results showed that 50% of the lanes exhibited linear structural behavior, while the remaining lanes demonstrated nonlinear structural behavior. Notably, the maximum deflections of all tested lanes were in compliance with AASHTO requirements.
- The lateral distribution of maximum deflection depicted that the source of bridge deck nonlinearity is due to potential problems in Prestressed Reinforced Concrete (PRC) girders.
- The flexural bridge rating indicated that the safe vehicle load that can be applied to the tested bridge is 72.9 tons.

ACKNOWLEDGEMENT

This work has been carried out in the Engineering College of Basrah University.

REFERENCES

[1] *The Manual of Bridge Evolution*, 3rd ed. Washington DC, USA: AASHTO, 2018.

[2] A. Huckelbridge and N. Capaldi, "Development of A Load Test for The Evaluation and Rating of Short-Span Reinforced Concrete Slab Bridges," Department of Civil Engineering, Case Western Reserve University, Ohio, USA, FHWA/OH-2002-012, 2002.

[3] *The Study on Capacity Development in Bridge Rehabilitation Planning, Maintained and Management Based on 29 Bridges of National Highway Network in Costa Rica*. Japan: Japan International Cooperation Agency (JICA), 2007.

[4] P. Bujňáková, J. Jošt, and M. Farbák, "Load testing of Highway Bridge," *MATEC Web of Conferences*, vol. 196, 2018, Art. no. 02020, https://doi.org/10.1051/matecconf/201819602020.

[5] R. de Vries, E. O. L. Lantsoght, R. D. J. M. Steenbergen, and M. Naaktgeboren, "Proof Load Testing Method by the American Association of State Highway and Transportation Officials and Suggestions for Improvement," *Transportation Research Record*, vol. 2677, no. 11, pp. 245–257, Nov. 2023, https://doi.org/10.1177/03611981231165026.

[6] A. B. Hassine, "A New Agent-based Solution for Bridge Lifespan Extension," *Engineering, Technology & Applied Science Research*, vol. 13, no. 3, pp. 10916–10921, Jun. 2023, https://doi.org/10.48084/etasr.5958.

[7] *Guidelines for the Supplementary Load Testing of Bridges*, 1st ed. London, UK: Thomas Telford Publishing, 1998.

[8] *FM 55-30, Army Motor Transport Operations*. Washington DC, USA: Department of the Army, 2013.

[9] "Bridge Design and Specifications," AASHTO LRFD, Washington DC, USA, FHWA-HRT-05-056, 2013.

[10] K. Witz, "Review of Applied Statistics for the Behavioral Sciences," *Journal of Educational Statistics*, vol. 15, no. 1, pp. 84–87, 1990, https://doi.org/10.2307/1164825.